CAGRA:
Occlusion-capable Automultiscopic 3D Display with Spherical Coverage

Yusuke Doyama, Tomohiro Taniakawa, Kazuyoshi Tagawa, Koichi Hirota and Michitaka Hirose
the University of Tokyo
7-3-1 Hongo, Bunkyo-ku, Tokyo 113-8656, Japan
{ydoya,tani,tagawa,hirose}@cyber.t.u-tokyo.ac.jp
hirota@media.k.u-tokyo.ac.jp

Abstract

This paper describes theory and implementation of a novel automultiscopic 3D display, CAGRA (Computer Aided Graphical Real-world Avatar), that provides spherical coverage and correct occlusion at the same time. CAGRA consists of two important ideas: rotating a mirror on two axes and switching images directionally at high speed. Mirror rotation on two axes enables the display to emit light to any direction in order to provide a 3D view for every viewpoint around it. Directional high-speed image switching is necessary to present different views for many viewpoints. We conducted an experiment on the prototype system of CAGRA, and proved that it presents a monochrome 3D view of a static object for 1250 viewpoints at 1[fps]. The experiment proved CAGRA is the first 3D display that is both spherically viewable from all around and capable of occlusion.

1. Introduction

Over the decades many types of 3D displays have been investigated, but they have not been widely accepted due to the physical and expressional constraints they impose on users. No 3D displays have ever provided a 3D view so realistic that users will stretch their arms to grab it before knowing it is merely an image. For example, HMDs[1, 2] attached in front of the users' eyes shut down the connection between the real world and users. In this respect, no matter how beautiful a 3D view they create, the view does not present reality as much as a view seen with the naked eyes. Although flat panel 3D displays[3, 4] present a 3D view to the naked eyes, their limited viewing angle prevent the view blend into background environment. This also reduces the reality of the view.

Our approach provides easier access to accurate and realistic 3D information, prticularly information such as the shape and position of imaginary 3D objects. We developed a new display, CAGRA, that can be used with naked eyes and is also able to transmit optically collect images all around it. CAGRA is categorized as a rotational 3D display. However, this system includes new ideas that solve the existing problems of rotational 3D displays. Key ideas in CAGRA are a rotating mirror on two axes and directional switching of images at high speed. Figure 1 shows the concept schematic of CAGRA.

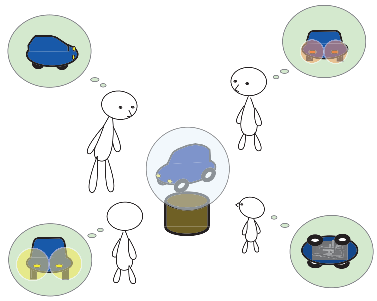

Figure 1. Concept schematic of CAGRA

CAGRA has the following features:

- **Presents 3D information for viewers at arbitrary positions.** Any user around the display can recognize a projected image regardless of their height and distance from the display. Users can observe all sides of a 3D view intuitively by moving their head and body, as if a real object exists inside the display.
- **Does not require special equipment.** Users need not wear goggles or attach positioning sensors to see the 3D view. They also need not to use input interfaces such as a mouse or a motion sensor to grasp all-around 3D information.
- **Shows images with occlusion.** Images expressing correct occlusion are projected for each viewpoint.

ICAT 2008
Dec. 1-3, Yokohama, Japan
ISSN: 1345-1278

Consequently, the displayed 3D view has a wider range of expression.

In this paper, at first we show the existing problems of rotational 3D displays by summarizing recent studies. Then, we propose the CAGRA system to solve these problems, and explain the details of the prototype system and evaluation experiments. Finally, we discuss the limitations at this stage and future work.

2. Related Work

Recently, rotational 3D displays are actively researched. The rotational 3D displays produce a 3D view by rotating a 2D display device, such as a liquid crystal display, a plasma display panel and a projection display. In other words, they demultiplex 2D images spatially. They provide a wide viewing angle, and do not require users to wear goggles or use other devices in order to present a 3D view. Thus, they can be easily introduced into an ordinary living environment or public space.

Rotational 3D displays are grouped into volumetric displays and automultiscopic displays. These two types of displays have advantages and disadvantages different from each other.

Volumetric displays A volumetric display creates light-emmiting points, or voxels, in the air by rotating pixels of a 2D display (See Figure 2). These voxels are seen from any viewpoints around the display, since they emit light into all direction. This means the display can present a 3D view to any viewpoint around the display. However, because of transparency of voxels, the display cannot present occlusion.

Brinkmann[5] developed a volumetric display with a spiral screen and laser array. Favalora et al.[6] constructed a system where high update-rate DMD projectors project images on a rotating diffuser screen. Aside from rotational displays, Kameyama et al.[7] built a linear scanning volumetric display.

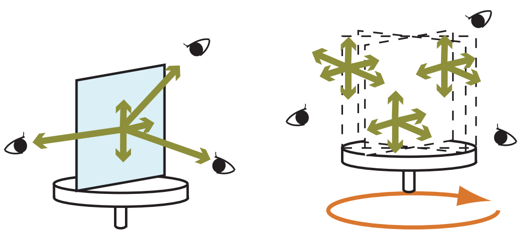

Figure 2. Volumetric Displays

Automultiscopic displays Automultiscopic displays switche 2D images at high speed according to the rotation angle (See Figure 3). The 2D display used in the automultiscopic display has narrow directivity so that each 2D image is presented for a limited part of the area around the display. The display can present correct occlusion for any viewpoints. However, with one axis of rotation, for example, it present correct parallax only on the plane of rotation. Thus, the positions of viewpoints to which the display presents correct parallax are limited to a small area.

Maeda et al.[8, 9] used two rotating tablet PCs with vertically oriented light-control film. Tanikawa et al.[10] further extended the system into a human-sized video avatar. Otsuka et al.[11] used a rotating screen with narrow directivity and a mirror with a projector, in order to split one frame of projector mirror. Jones et al.[12] and Cossairt et al.[13] developed sophisticated systems using an altered DMD projector and rotating directional screen. Yendo et al.[14] also develped a rotational auto-multiscopic display that uses 1D vertical arrays of LEDs and rotational parallax barrier, although its operation principle is different from the explanation above.

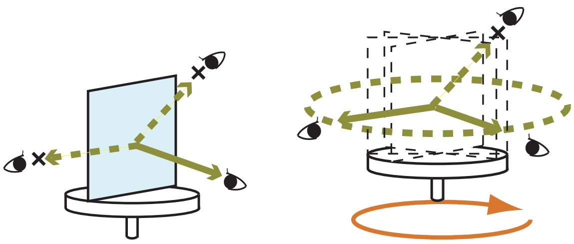

Figure 3. Automultiscopic Displays

3. Design Proposal

As described in Section 2, volumetric displays provide 3D views toward all direction. However, the displayed views can not present occlusion due to a methodological reason. On the other hand, automultiscopic displays are able to present occlusion-capable images for any viewpoints, but position of each viewpoint is limited to certain area. Therefore, we developed the novel automultiscopic 3D display CAGRA, which provides an occlusion-capable 3D view for viewpoints around the display.

Figure 4 shows two important ideas of this display: switching images directionally at high speed and rotating a mirror on two axes. CAGRA adopts a two-sided mirror with a holographic diffuser on the surface. The holographic diffuser enables the mirror to act as a screen with narrow directivity. This characteristic leads to independence of nearby viewpoints. By projecting numerous 2D images from above toward the mirror at high speed, the mirror projects many different images toward a limited area around the display. Furthermore, CAGRA rotates the mirror on two axes or-

ICAT 2008
Dec. 1-3, Yokohama, Japan
ISSN: 1345-1278

thogonal to each other, so that it can direct the surface of the mirror to any direction. By rotating the mirror on two axes, the projected 2D images are reflected toward all around the display. This is necessary to allocate viewpoints all around the display. With these two ideas combined, CAGRA can provide spherical coverage and correct occlusion simultaneously. In other words, it is capable of showing occlusion as well as viewable from all around the display. Figure 5 shows how CAGRA works.

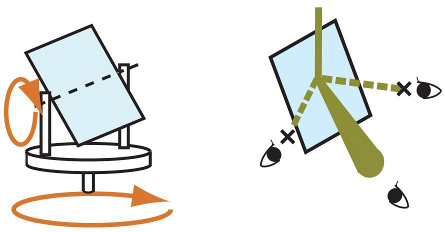

Figure 4. Left: Rotating a mirror on two axes, Right: Switching images directionally

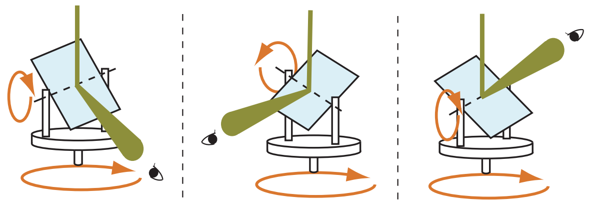

Figure 5. Concept of CAGRA

3.1. Two-axis Mirror Rotation

Figure 6 shows a model of the two-axis rotation. If the light is projected from above ($\phi = 0$), the relationship between the mirror position α, β and the viewpoint position (θ, ϕ) is expressed as $\theta = \alpha$, $\phi = 2\beta$. Therefore, assuming that $\dot{\alpha} = \omega_\alpha$ *(const)*, $\dot{\beta} = \omega_\beta$ *(const)*, viewpoint position (θ, ϕ) at time t is expressed as

$$\theta = \omega_\alpha t \tag{1}$$

$$\phi = 2\omega_\beta t \tag{2}$$

On the basis of these two equations, the movement of the viewpoint orbit can be calculated. Figure 7 shows the intersection orbit of the sphere and the light ray that comes from above the mirror and is reflected at the center of the mirror. The simulation was carried out under the condition $\omega_\alpha = 22\pi$[rad/sec]. $\omega_\beta = 20\pi$[rad/sec]. The orbit of a viewpoint is a certain locus defined by $\omega_\alpha, \omega_\beta$.

The resulting orbit have similar characteristics to Lissajous' curve. We define the slope of the orbit γ and the

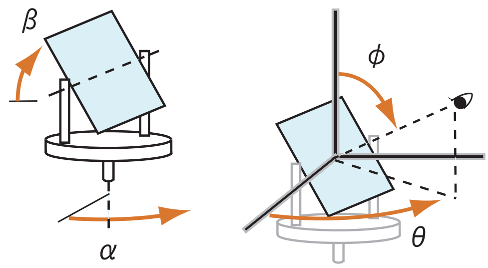

Figure 6. Standard coordinates. Left:Mirror position, Right: Viewpoint position

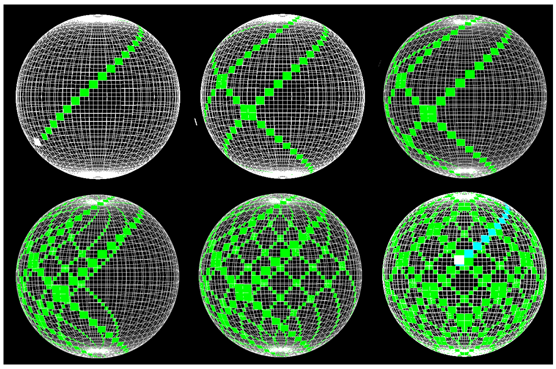

Figure 7. Timeline change of the orbit under the condition $\omega_\alpha = 22\pi$[rad/sec], $\omega_\beta = 10\pi$[rad/sec]

viewpoint speed v as

$$\gamma = tan^{-1}\left(\frac{2\omega_\beta}{\omega_\alpha}\right) \tag{3}$$

$$v = \sqrt{\omega_\alpha^2 + (2\omega_\beta)^2} \tag{4}$$

γ affects shape of the orbit. v affects rotation cycle of the orbit, provided that γ is constant.

Figure 8 shows the relationship between γ and the shape of the orbit. The left side of Figure 8 shows the simulation result under the condition $\omega_\alpha = 6\pi$[rad/sec], $\omega_\beta = 8\pi$[rad/sec]. By applying Equation 3, we obtain $\gamma = 1.21$. The right side of Figure 8 shows the result under the condition $\omega_\alpha = 22\pi$[rad/sec], $\omega_\beta = 10\pi$[rad/sec]. By applying Equation 3, we obtain $\gamma = 0.73$. When the orbit become denser, the number of viewpoints increases. But denser orbit means large length of the orbit, resulting in lower refresh rate.

Figure 9 shows the relationship between v and rotation cycle of the orbit when γ is the same value. The left side of Figure 9 shows the simulation result under the condition $\omega_\alpha = 6\pi$[rad/sec], $\omega_\beta = 8\pi$[rad/sec]. The right side of Figure 9 shows the result under the condition $\omega_\alpha = 12\pi$[rad/sec], $\omega_\beta = 16\pi$[rad/sec]. Refresh rate for each viewpoint of the simulation result on the right is twice as

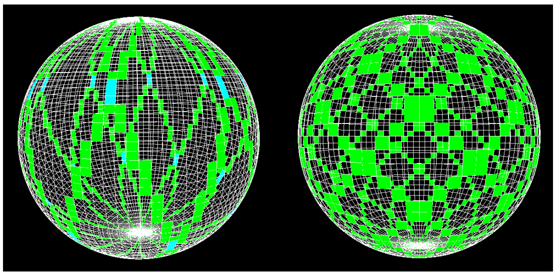

Figure 8. Relationship between γ and shape of the orbit. Left: $\gamma = 1.21$, Right: $\gamma = 0.73$

large as that of the simulation result on the left. This means larger v is preferable, although the possible value of v is affected with mechanical constraints.

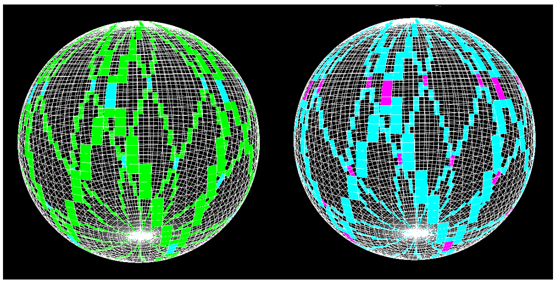

Figure 9. Relationship between v and cycle of the orbit. Left: $\gamma = 1.21$, $v = 17.08\pi$, Right: $\gamma = 1.21$, $v = 34.17\pi$

3.2. Directional Image Switching

Actually, our system comprises a combination of a mirror and a holographic diffuser, which acts as a screen with narrow directivity. Figure 10 shows the result of orbital simulation when effect of the holographic diffuser is taken into account. The filled area on the sphere is the intersection of the sphere and the light ray that was reflected at the center of the mirror and diffused by the effect of the holographic diffuser. With the holographic diffuser, the margin of orbit is filled and effectively covers the entire area of the sphere around the display. However, the holographic diffuser also causes overlap of the projected image.

3.3. Parameter Relationship

Given that projector refresh rate f and orbit cycle T, number of viewpoints N and refresh rate for each viewpoints F can be expressed by

$$F = \frac{1}{T} \tag{5}$$

$$N = fT \tag{6}$$

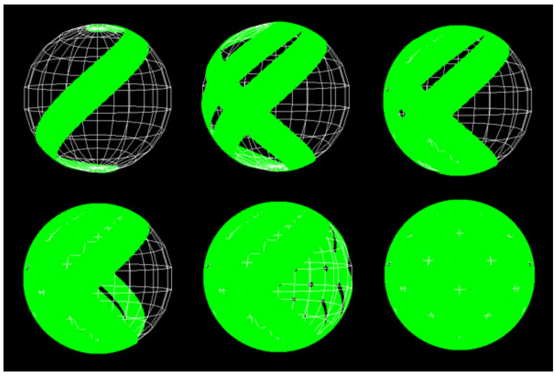

Figure 10. Simulation result with the effect of the diffusion under the condition $\omega_\alpha = 22\pi$[rad/sec], $\omega_\beta = 10\pi$[rad/sec], diffusion angle of holographic diffuser is 10.0[deg]

By eliminating T, these equation become $f = FN$. This shows trade-off relationship between F and N. In order to get F and N large enough, it is important to set f as large as possible. Thus, high-speed image switching is important.

T is determined by ω_α and ω_β. In other words, T is affected by v and γ, the shape of the orbit.

4. Overview of the Prototype System

From the structural point of view, the prototype system is divided into two parts: a rotation unit and a projection unit. Although these two units are preferable to be synchronized, they are independent while running in this prototype system.

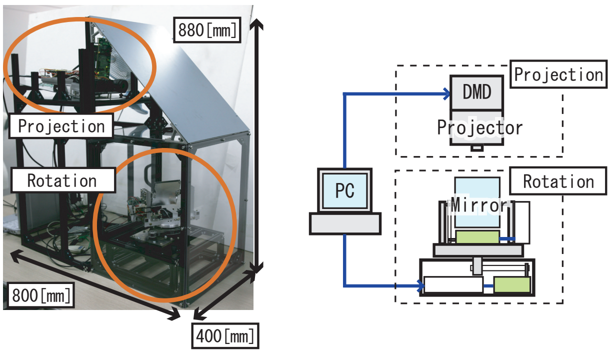

Figure 11. Left:Appearance of display, Right: System overview

4.1. Rotation Unit

Figure 12 shows the appearance of the rotation unit. The rotation unit is further divided into a mirror-rotation structure and a base-rotation structure. In the mirror-rotation structure, the rotating mirror is two sided and consists of two acrylic mirrors that are connected at the back (Figure 13). The shaft is located between these two acrylic mirrors.

In order to reduce the moment of inertia, acrylic mirrors was adopted instead of glass mirrors. The size of the mirror is 100x100[mm]. Holographic diffusers with a 5[deg] diffusion angle are placed on the surface of the mirror. As the projected light comes to the mirror, reflects on the surface and goes out to somewhere, the light passes through the diffuser twice. Thus, the overall diffusion angle of this mirror is estimated to be about 10[deg]. The mirror-rotation structure is located on the base-rotation structure, connecting only electric power cables. As mentioned already, the axis of mirror rotation and the axis of base rotation are orthogonal to each other. Size of the rotation base structure is 300[mm] x 300[mm] x 180[mm].

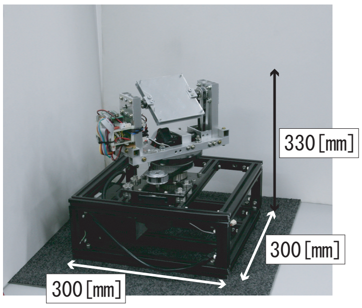

Figure 12. Appearance of Rotation unit

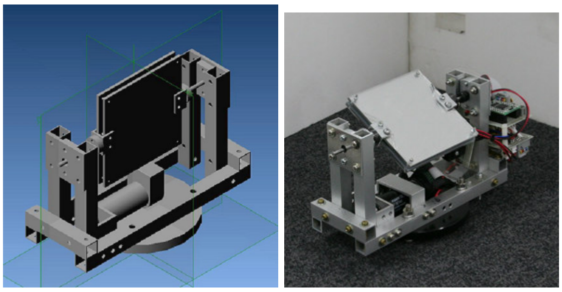

Figure 13. Mirror rotation structure. Left: Schematic, Right: Appearance

4.2. Projection Unit

We adjusted an commercially available projector in order to obtain a high refresh rate. We used a DMD Discovery 3000 board from Texas Instrument Inc. The Discovery board enables users to control the DMD chip directly. We also used an ALP-3 daughter board from Valuax Inc. The daughter board enables the control computer to store images in its memory via a USB connection. The Discovery board with the daughter board is able to store 1365 XGA-sized monochrome images. The maximum refresh rate is 13,333[Hz].

The control computer renders profile images of the 3D object in advance, and stores the prerendered profile images in the memory of the DMD board. The images were processed into 1-bit monochrome images by Floyd-Steinberg dithering, because a high refresh rate is more important than color depth in this system. The images stored on the memory are projected to the loop at the refresh rate set by the control computer. The refresh rate of the projector can be set in microsecond order.

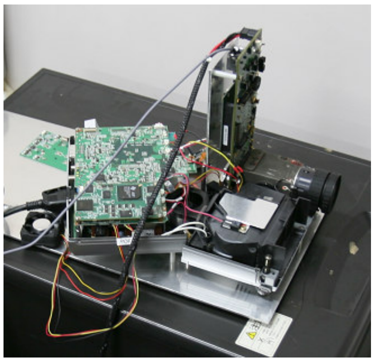

Figure 14. Appearance of projection unit

5. Experiment

5.1. Conditions

We conducted an experiment to evaluate the display. ω_α and ω_β were set at 6π[rad/sec] and 16π[rad/sec] respectively. Figure 15 shows a result of the viewpoint orbit simulation under this condition. 1250 images sized 1024x768[pixels] were presented at the speed of 1250[fps]. Figure 16 shows part of pre-rendered images. 2D images was created from 3D model of a teapot drawn with OpenGL. Based on the discussion in Section 3, ω_α and ω_β give refresh rate for each viewpoints F and the number of viewpoints N. When $\omega_\alpha = 6\pi$[rad/sec] and $\omega_\beta = 16\pi$[rad/sec], $T = 1$[sec]. By applying Equation 5, 6, F and N are calculated to be 1[fps] and 1250.

In order to project correct images for each viewpoint, image and mirror position (α, β) is interrelated. However, we have not implemented automatic synchronization system yet. This time we adjusted relationship between image and the mirror position manually.

5.2. Result

Figure 17 shows the result of the experiment. A presented view was static for a certain viewpoint. The display presented horizontal parallax for 360[deg]. It also presented vertical parallax as far as the view is not disturbed by structure of the prototype system. The display was also able to

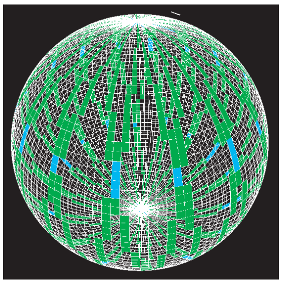

Figure 15. Simulation result of the viewpoint orbit under the condition $\omega_\alpha = 6\pi$[rad/sec], $\omega_\beta = 16\pi$[rad/sec]

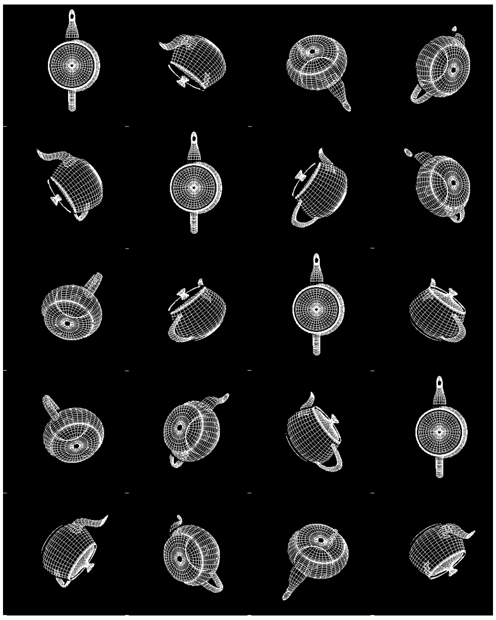

Figure 16. Part of projected images. Each image is associated with certain viewpoint.

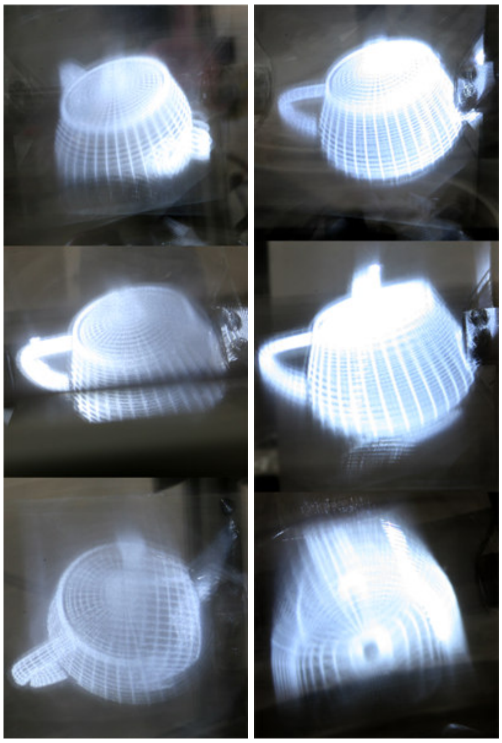

Figure 17. Result of the experiment. Left: Horizontal, Right: Vertical

show occlusion. As a result, 3D structure of teapot was easily recognized.

6. Discussion and Future Work

There are several points for further development of CAGRA. Firstly, projected 2D images needs compensation for the narrow directivity of mirror with the holographic diffuser, which is introduced for filling margins of the viewpoint orbit. 2D images are projected under the assumption that a position of the mirror and a 2D image have an one-to-one relationship. The assumption means whole part of a projected image is observable from each of viewpoints at one time. Due to the effect of narrow directivity coming from holographic diffuser, however, only limited part of the image are observable from some viewpoint at one time. This means projected 2D images need to be compensated. Multiple Center of Projection image[15] is the solution to this problem. We are now implementing this technique in our system.

Careful consideration on the orbit design is also necessary in order to realize stereoscopic vision with spherical coverage. As discussed in Section 3, the characteristics of CAGRA, such as refresh rate and the number of viewpoints, depend on its viewpoint orbits. For more precise analysis, the effect of diffusion by holographic diffuser, size of mirror and amount of reflection light have to be taken into consideration.

We have to improve refresh rate of the display to avoid a flicker. Refresh rate is up to rotation speed of mirror and the number of projection points. To increase rotation speed, improvement of mechanical structure is necessary. To increase the number of projection points, there are two options. The one is to increase the number of projector. The other is to split one image into several images with mirrors [11]. Though relationship between rotation and projection becomes much more complex as the number of projection points increases, simulation of the viewpoint orbit is still possible.

For various application use, the ability to show motion and colors are necessary. One way to present movie is putting DVI signal directly into DMD board [13]. This method also enables real-time interaction with a 3D object in the display. In order to show color, 3DMD method is available [6]. This method uses three DMD chips, assigning these chips for each of RGB colors. This means one frame consists of 3bit color image. Dithering makes the image look much more color for human eyes.

7. Conclusion

In this paper, we proposed the novel 3D display CAGRA, which consists of two-axis mirror rotation and high-speed directional image switching. At first we proved that combination of these ideas creates viewpoints all around the display. Then we discussed basic characteristics of the display, especially characteristics of the viewpoint orbit, which was determined by rotation speed of the mirror and the base. Based on these discussion, we implemented a prototype system. Evaluation of the prototype system proved CAGRA is the first 3D display that can provide spherical coverage and occlusion at the same time. Finally we discussed points to improve and possible solutions. The ultimate goal of CAGRA is to create an easy-to-use 3D display that produce perfect light field of a 3D object.

8. Acknowledgement

The authors are deeply grateful to Hiroki Kobayashi for his enormous support and insightful comments on this paper. Special thanks also go to Atsushi Kodama, who helped to carry out experiments. I would like to thank Kunihiro Nishimura and Jun'ichi Nakano for invaluable comments during the course of my study. This work is sponsored by MEXT-JST Digital Public Art project.

References

[1] I.E.Sutherland, A HEAD-MOUNTED THREE-DIMENSIONAL DISPLAY. *Proc. the Fall Joint Computer Conference*, pp. 757-764, 1968. 1

[2] K.Kiyokawaa, Y.Kurata and H.Ohno, An optical see-through display for mutual occlusion with a real-time stereovision system, *Computers and Graphics*, Vol. 25, Issue 5, pp. 765-779, 2001. 1

[3] H.Liao, M.Iwahara, N.Hata, I.Sakuma, T.Dohi, T.Koike, Y.Momoi, T.Minakawa, M.Yamasaki, F.Tajima and H.Takeda, High-resolution integral videography autostereoscopic display using multi-projector. *Proc. the Ninth International Display Workshops*, Vol. 12, Issue 6, pp. 1067-1076, 2002. 1

[4] S.Nakajima, K.Nakamura, K.Masamune, I.Sakuma and T.Dohi, Three-dimensional medical imaging display with computer-generated integral photography, *Computerized Medical Imaging and Graphics*, Vol. 25, Issue 3, pp. 235-241, 2001. 1

[5] U.Brinkmann, A Laser-Based Three-Dimensional Display, *Lasers and Applications*, pp. 55-56, 1983. 2

[6] G.E.Favalora, J.Napoli, D.M.Hall, R.K.Dorval, M.Giovinco, M.J.Richmond, W.S.Chun, 100-million-voxel volumetric display, *Proc. SPIE*, 4712, pp. 300-312, 2002. 2, 7

[7] K.Kameyama, K.Ohtomi and Y.Fukui, A Virtual Reality System Using a Volume Scanning 3D Display, *Proc. ICAT 92*, pp.49-62, 1992. 2

[8] H.Maeda, K.Hirose, J.Yamashita, K.Hirota and M.Hirose, All-Around Display for Video Avatar in Real World, *Proc. The Second IEEE and ACM International Sysmposium on Mixed and Augumented Reality (ISMAR03)*, pp. 288-289, 2003. 2

[9] H.Maeda, T.Tanikawa, J.Yamashita, K.Hirota and M.Hirose, Real world vido avatar: transmission and presentation of human figure, *Proc. IEEE VR 2004*, pp 237-238, 2004. 2

[10] T.Tanikawa, Y.Suzuki, K,Hirota and M.Hirose, Real World Video Avatar: Real-time and Real-size Transmission and Presentation of Human Figure, *Proc. ICAT 2005*, pp 112-118, 2005. 2

[11] R.Otsuka, T.Hoshino, and Y.Horry, Transpost: A novel approach to the display and transmission of 360 degrees-viewable 3d solid images, *IEEE TRANSACTIONS ON VISUALIZATION AND COMPUTER GRAPHICS*, Vol. 12, No. 2, pp. 178-185, 2006. 2, 6

[12] O.S.Cossairt, J.Napoli, S.L.Hill, R.K.Dorval and G.E.Favalora. Occlusion-capable multiview volumetric three-dimensional display, *APPLIED OPTICS*, Vol. 46, No. 8, pp. 1244-1250, 2007. 2

[13] A.Jones, I.McDowall, H.Yamada, M.Bolas, and P.Debevec. Rendering for aninteractive 360deg light field display. In *SIGGRAPH 2007*, volume 26, 2007. 2, 6

[14] T.Yendo, N.Kawakami and S.Tachi, Seelinder: the cylindrical lightfield display, *Proc. SIGGRAPH 2005 emerging technologies*, article no.16, 2005. 2

[15] P.Rademacher and G.Bishop, Multiple-center-of-projection images, *Proc. the 25th annual conference on Computer graphics and interactive techniques*, pp. 199-206, 1998. 6